



Originally published as:

Göttl, F., F. Seitz: Contribution of non-tidal oceanic mass variations to polar motion determined from space geodesy and ocean data. In: Observing our Changing Earth, Sideris, M. (Ed.), IAG Symposia, Vol. 133, 439-446, Springer, Berlin, 2008.

DOI: [10.1007/978-3-540-85426-5_53](https://doi.org/10.1007/978-3-540-85426-5_53)

Contribution of non-tidal oceanic mass variations to polar motion determined from space geodesy and ocean data

Franziska Göttl

Deutsches Geodätisches Forschungsinstitut (DGFI), Alfons-Goppel-Strasse 11, D-80539 Munich, Germany; e-mail: goettl@dgfi.badw.de

Florian Seitz

Earth Oriented Space Science and Technology (ESPACE), Technische Universität München, Arcisstr. 21, D-80290 Munich, Germany

Abstract. In order to assess the contribution of non-tidal oceanic mass changes to polar motion, equatorial oceanic excitation functions are determined from combinations of space geodetic techniques and ocean data. Satellite altimetry provides accurate information on sea level anomalies (SLA) which are caused by mass and volume changes of seawater. In order to infer oceanic contributions to Earth rotation, the volume effect (steric effect) has to be reduced from the observations since Earth rotation is solely affected by mass variations. The steric effect is estimated from ocean state variables as a function of depth. Oceanic polar motion excitations from reduced SLA are compared with respective results from ocean models. Contributions of ocean currents, atmospheric and hydrological effects are added in order to validate the oceanic excitations from altimetry with independent geodetic observations which reflect the integral effect of a multitude of geophysical processes in the Earth system. This requires an investigation of accuracy and consistency of the combined data sets. The study reveals that model-only combinations of atmospheric, oceanic and hydrological excitations agree better with geodetic observations than combinations which include excitations from altimetry. Possible reasons could be errors in the steric reduction of SLA and/or the compensation of erroneous patterns in atmosphere data by numerical ocean models.

Keywords. oceanic mass variations, polar motion, satellite altimetry, steric effect

1 Introduction

Observation techniques of the motion of the Earth rotation axis with respect to the Earth's

surface have continuously improved over the last decades. While optical astrometry allowed for observations of polar motion with an accuracy of about one meter, modern space geodetic techniques such as Very Long Baseline Interferometry (VLBI), Satellite Laser Ranging (SLR) and Global Navigation Satellite Systems (GNSS) provide results at a millimetre level. However the geophysical interpretation of the time series in terms of contributions from particular geodynamic processes is a big challenge since the observations reflect the integral effect of redistribution and motion of masses within and between the individual subsystems of the Earth. Large effort has been made in the assessment of mass transports in atmosphere, hydrosphere and solid Earth in interdisciplinary research from geophysical modelling as well as from terrestrial and space borne observations.

Strictly speaking, geodetic observations of polar motion reflect the motion of the Earth rotation axis with respect to the Terrestrial Reference Frame (TRF). Consequently systematic errors in TRF computations might show up as artificial signals in polar motion time series. Therefore an improved geophysical understanding of dynamic processes and their interactions is important in order to obtain independent estimates of Earth rotation variations.

In this article we discuss results of oceanic polar motion excitation functions which have been derived from satellite altimetry observations. Different data sets for the reduction of steric sea level variations (volume changes due to changes of temperature and salinity) are applied in order to separate the effect of ocean mass redistributions from sea level anomalies as observed by Topex/Poseidon Extended Mission.

The oceanic mass excitations are subsequently compared with respective time series from the ocean models OMCT (Ocean Model for Circulation and Tides) and ECCO (Estimating the Circulation and Climate of the Ocean). Further we compare the total effect of atmospheric, oceanic and hydrological excitations with the geodetic observations of polar motion provided by International Earth Rotation and Reference Systems Service (IERS) in its C04 series. The comparisons will be performed for model-only combinations as well as for combinations in which the oceanic mass effect is derived from altimetry.

2 Data sources

All analyses in this study are performed on the basis of polar motion excitation functions. Excitation functions are the mathematical description of geophysical effects on Earth rotation. They comprehend angular momentum variations due to changes of the Earth's inertia tensor (mass term) and due to motions of masses with respect to the reference frame (so-called relative angular momenta; motion term). The advantage of an evaluation in the excitation domain is the absence of free oscillations of the Earth such as the Free Core Nutation and the Chandler oscillation.

2.1 Oceanic polar motion excitations

Oceanic polar motion excitations are determined from combinations of satellite altimetry and ocean data from hydrographical observations and models. Satellite altimetry provides accurate information on sea level anomalies (SLA) w.r.t a mean sea surface which are caused by mass and volume changes of seawater. At Deutsches Geodätisches Forschungsinstitut (DGFI) SLA are estimated from observations of the TOPEX/Poseidon Extended Mission which have been reduced by environmental and geophysical effects such as troposphere, ionosphere, sea state bias and tides. Additionally the classical inverse barometer (IB) correction has been applied. The latter accounts for the hydrostatic response of the ocean surface to atmospheric pressure variations. SLA are provided with a temporal resolution of 10 days. They are averaged to monthly mean fields in order to be consistent with other data sets as explained below.

As mentioned above Earth rotation is affected by mass variations but not by volume changes

of seawater. Therefore the steric effect has to be reduced from observed SLA. It is estimated from physical ocean parameters such as temperature and salinity changes in different depth layers of the ocean. Fofonoff and Millard (1983) give a detailed explanation about transient density anomalies using the equation of state of seawater. Vertical integration of density anomalies within a water column yield steric sea level variations; for details see Chambers (2006). Here we apply numerical corrections of the steric effect as provided from Ishii et al. (2006). Alternatively we use monthly three dimensional temperature and salinity fields which are based on objective analyses. They are offered from the National Oceanographic Data Centre (NODC) as parameters of the World Ocean Atlas 2005 (WOA05) (Antonov et al. (2006); Locarnini et al. (2006)).

After the steric corrections have been applied, the reduced SLA are interpreted as oceanic mass signals which are expressed in equivalent water heights (EWH). Those are subsequently converted into polar motion excitations (mass term) χ_1^O and χ_2^O (units: rad = $\frac{180^\circ}{\pi} \cdot 3600 \cdot 1000$ mas) by

$$\left. \begin{aligned} \Delta \bar{C}_{nm}^{ewh} \\ \Delta \bar{S}_{nm}^{ewh} \end{aligned} \right\} = \frac{1}{4\pi} \int_0^{2\pi} \int_0^\pi \Delta ewh_Q \bar{P}_{nm}(\cos \theta_Q) \cdot \left. \begin{aligned} \cos m\lambda_Q \\ \sin m\lambda_Q \end{aligned} \right\} \sin \theta_Q d\theta_Q d\lambda_Q, \quad (1)$$

$$\left. \begin{aligned} \Delta \bar{C}_{nm} \\ \Delta \bar{S}_{nm} \end{aligned} \right\} = \frac{1}{2n+1} \cdot \frac{3\rho_w}{R\bar{\rho}_e} \left. \begin{aligned} \Delta \bar{C}_{nm}^{ewh} \\ \Delta \bar{S}_{nm}^{ewh} \end{aligned} \right\} \quad (2)$$

and

$$\left. \begin{aligned} \chi_1^O \\ \chi_2^O \end{aligned} \right\} = -0.684 \cdot \frac{1.608 R^2 M_e}{C-A} \cdot \sqrt{\frac{5}{3}} \cdot \left. \begin{aligned} \Delta \bar{C}_{21} \\ \Delta \bar{S}_{21} \end{aligned} \right\} \cdot (3)$$

In these equations $\Delta \bar{C}_{nm}^{ewh}$ and $\Delta \bar{S}_{nm}^{ewh}$ denote normalized coefficients of the spherical harmonic expansion of the EWH (units: m). $\Delta \bar{C}_{nm}$ and $\Delta \bar{S}_{nm}$ are dimensionless normalized Stokes coefficients; λ_Q and θ_Q stand for the spherical geocentric coordinates of the integration point Q; $\bar{P}_{nm}(\cos \theta_Q)$ denote the fully normalized Legendre functions of degree n and order m ; $\rho_w = 1000$ kg m⁻³ is the density of fresh water, $\bar{\rho}_e = 5517$ kg m⁻³ is the average density of the Earth and $R = 6378136.46$ m its mean radius.

In Eq. (3) the factor $0.684 = 1 + k'_2 + \Delta k'_{an}$ explains the effect of the yielding of the Earth's

body to surface loads where $k'_2 = -0.305$ is the solid Earth load Love number of degree 2 and $\Delta k'_{an} = -0.011$ accounts for the effects of mantle inelasticity. The factor $1.608 = [\Omega(C - A)] / [(C - A + A_m + \epsilon_C A_C) \sigma_0]$ comprehends the effects of core-mantle decoupling and rotational deformation (Gross (2007); Chen et al. (2000)).

Numerical values are: $\Omega = 7.292115 \cdot 10^{-5}$ rad s⁻¹ (mean angular velocity of the Earth), $C = 8.0365 \cdot 10^{37}$ kg m² and $A = 8.0101 \cdot 10^{37}$ kg m² (axial and equatorial moments of inertia), $A_m = 7.0999 \cdot 10^{37}$ kg m² (equatorial moment of inertia of the mantle), $A_C = 9.1168 \cdot 10^{36}$ kg m² (equatorial moment of inertia of the core), $\epsilon_C = 2.546 \cdot 10^{-3}$ (ellipticity of the core) and $\sigma_0 = 2\pi / (434.2 \cdot 86164)$ rad s⁻¹ (observed Chandler frequency).

Resulting oceanic excitation functions χ_1^O and χ_2^O are compared with respective time series from the ocean models ECCO and OMCT. The Special Bureau for the Oceans (SBO) of the Global Geophysical Fluids Centre (GGFC) provides six-hourly series of OAM (oceanic angular momenta; mass term) and oam (motion term) computed from the ECCO run kf049f (Gross et al. (2003)). The model is forced by wind stress, heat and freshwater fluxes from the atmospheric reanalyses of NCEP/NCAR (National Centres for Environmental Prediction/ National Centre for Environmental Research) (Kalnay et al. (1996)); an exact inverse barometric response of the ocean surface to atmospheric pressure variations is assumed. ECCO assimilates altimetry and Expendable Bathythermograph (XBT) data. Further information can be found in Gross et al. (2005). Besides we use six-hourly OAM- and oam-series computed from OMCT (Thomas et al. (2001)). This model is forced by wind stress, 2m-temperature and freshwater fluxes from the operational analysis of the ECMWF (European Centre for Medium-Range Weather Forecasts). Like in ECCO no atmospheric pressure forcing is taken into account in the applied OMCT version.

To be consistent with the results from altimetry the modelled OAM- and oam-series are averaged into monthly mean values. Oceanic polar motion excitations χ_1^{ocean} and χ_2^{ocean} (units: rad) are computed from

$$\left. \begin{matrix} \chi_1^O \\ \chi_2^O \end{matrix} \right\} = 0.684 \cdot \frac{1.608}{\Omega(C - A)} \cdot \left\{ \begin{matrix} OAM_1 \\ OAM_2 \end{matrix} \right\}, \quad (4)$$

$$\left. \begin{matrix} \chi_1^o \\ \chi_2^o \end{matrix} \right\} = \frac{1.608}{\Omega(C - A)} \cdot \left\{ \begin{matrix} oam_1 \\ oam_2 \end{matrix} \right\} \quad (5)$$

and

$$\left. \begin{matrix} \chi_1^{ocean} \\ \chi_2^{ocean} \end{matrix} \right\} = \left\{ \begin{matrix} \chi_1^O + \chi_1^o \\ \chi_2^O + \chi_2^o \end{matrix} \right\}. \quad (6)$$

Figure (1) displays equatorial oceanic mass excitation functions from reduced SLA and the ocean models. Especially in χ_1 significant discrepancies are obvious. Correlation coefficients between all displayed curves range from 0.18 to 0.77 for χ_1 and from 0.45 to 0.87 for χ_2 , where the highest values occur between the two solutions from reduced SLA.

The corresponding RMS differences range from 4.1 to 8.5 mas for χ_1 and from 4.7 to 8.0 mas for χ_2 . While the range of the values of the curves, i.e. approximately ± 20 mas in both components, represents the absolute contribution of the oceanic mass term to polar motion excitation, the RMS values are related to the uncertainty of this geophysical effect.

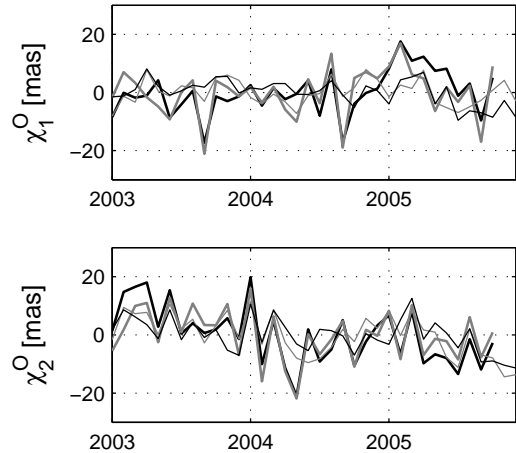


Fig. 1 Solutions for equatorial oceanic mass excitation from reduced SLA (steric reductions from Ishii (grey fat line) and from WOA05 (black fat line)) and from the models ECCO (grey thin line) and OMCT (black thin line). A mean value for the period between 2003 and 2005 is subtracted from each of the time series.

The results of the oceanic mass excitation functions from altimetry shall be compared to precise geodetic observations of polar motion. However there is no direct measure for the oceanic contribution since the observations reflect the integral effect of mass and motion terms of a multitude of geophysical processes. The

largest effects are due to mass transports in the atmosphere, the oceans and the continental hydrosphere. Consequently atmospheric and hydrological effects as well as the oceanic motion term must be either removed from the geodetic observations or - vice versa - added to the oceanic mass effect in order to achieve comparable time series. In the following we will deal with the latter possibility.

2.2 Atmospheric polar motion excitations

Atmospheric angular momentum time series AAM (mass term) and aam (motion term) due to pressure changes and winds are provided from the NCEP reanalyses by the Special Bureau for the Atmosphere (SBA) of the GGFC. The time series are available with a temporal resolution of six hours. Since the effect of atmospheric pressure forcing is excluded in all oceanic data sets an IB correction has been adopted, i.e., atmosphere pressure variations have been set to zero over the oceans (Zhou et. al. (2006)). In the framework of the DFG (Deutsche Forschungsgemeinschaft) research unit FOR584 "Earth Rotation and Global Dynamic Processes" AAM and aam-series from six-hourly operational ECMWF analyses are available. Like in the case of NCEP an IB correction has been adopted.

The AAM and aam-series are averaged into monthly mean values and converted into atmospheric polar motion excitations χ_1^{atmo} and χ_2^{atmo} (units: rad) by

$$\left. \begin{matrix} \chi_1^A \\ \chi_2^A \end{matrix} \right\} = 0.684 \cdot \frac{1.608}{\Omega(C-A)} \cdot \begin{Bmatrix} AAM_1 \\ AAM_2 \end{Bmatrix}, \quad (7)$$

$$\left. \begin{matrix} \chi_1^a \\ \chi_2^a \end{matrix} \right\} = \frac{1.608}{\Omega(C-A)} \cdot \begin{Bmatrix} aam_1 \\ aam_2 \end{Bmatrix} \quad (8)$$

and

$$\left. \begin{matrix} \chi_1^{atmo} \\ \chi_2^{atmo} \end{matrix} \right\} = \begin{Bmatrix} \chi_1^A + \chi_1^a \\ \chi_2^A + \chi_2^a \end{Bmatrix} \quad (9)$$

Figure (2) displays the combined effect of mass and motion term of the atmospheric polar motion excitation functions. Both signals are very similar and feature high correlation coefficients that amount to 0.70 for χ_1 and 0.98 for χ_2 . Comparatively small RMS values for χ_1 (5.8 mas) and χ_2 (4.1 mas) indicate a low uncertainty of the equatorial atmospheric excitation functions, i.e., the atmospheric effect is known much better than the oceanic one. The curves of χ_2 are characterised by significantly larger amplitude variations (values between -59 and 35 mas) than the

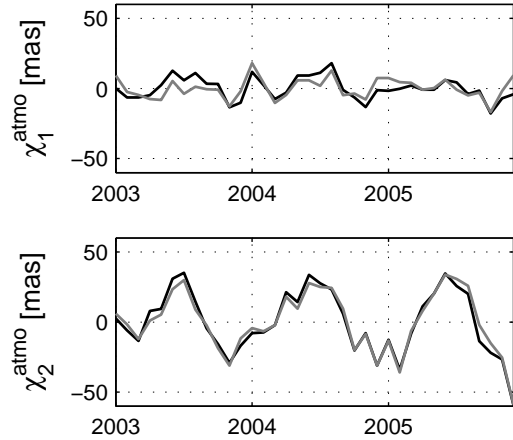


Fig. 2 Atmospheric excitation functions of polar motion (mass and motion term) from NCEP (black) and ECMWF (grey). A mean value for the period between 2003 and 2005 is subtracted from both time series.

curves of χ_1 (values between ± 18 mas). This can be explained by the geographical dependency of the excitation functions. Regions in which mass redistributions have a large influence on χ_2 are located along the $\pm 90^\circ$ -meridians which cross the major landmasses of Eurasia and North and South America. In contrast χ_1 is mainly influenced by mass variations around the 0° and 180° -meridians which cross the Atlantic and the Pacific ocean. Since atmospheric pressure changes are set to zero over the oceans due to the IB correction, the contributions are much smaller in this component.

2.3 Hydrological polar motion excitations

Hydrological excitation functions are computed from monthly fields of global water storage variations. Respective data sets from the model LDAS (Land Data Assimilation System) developed at National Oceanic and Atmospheric Administration (NOAA) Climate Prediction Centre (CPC) are provided in monthly resolution by the Special Bureau for Hydrology (SBH) of the GGFC. Furthermore we derived monthly fields of EWH changes from surface water, groundwater and snow from the LaD (Land Dynamics) model (Milly and Shmakin, 2002). Modelled water storage variations are transformed into hydrological polar motion excitations χ_1^H and χ_2^H (units: rad) following Eq. (1) to (3).

Currently no hydrological relative angular momentum series are offered by the SBH because of existing model deficiencies. However the motion effect is very small because of the comparatively slow transport processes of continental water masses.

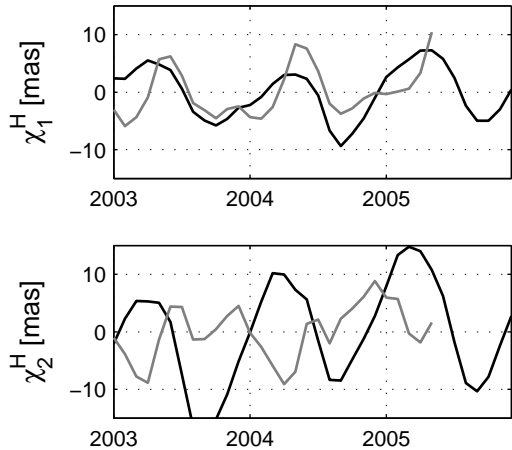


Fig. 3 Excitation functions of polar motion due to mass redistributions within the continental hydrosphere (LDAS: black; LaD: grey). A mean value for the period between 2003 and 2005 is subtracted from both time series.

Figure (3) compares the hydrological mass excitation functions of polar motion from both models. The curves feature very large discrepancies which are also reflected by the correlation coefficients which amount to 0.57 for χ_1 and -0.22 for χ_2 . Especially the curves of χ_2 show poor agreement and they are even out of phase. The RMS differences between the curves are 4.2 mas for χ_1 and 10.9 mas for χ_2 . Consequently the hydrological mass effect causes a similar uncertainty in the total equatorial excitations as the oceanic mass effect.

3 Validation of the integral effect with geodetic observations

We compare consistent combinations of the above data sets with the integral effect from independent geodetic observations:

[1] atmospheric effect from ECMWF combined with the oceanic mass effect from altimetry (steric reduction from WOA05) and the oceanic motion effect from OMCT;

[2] atmospheric effect from ECMWF combined with the oceanic mass effect from altimetry

(steric reduction from Ishii et al. (2006)) and the oceanic motion effect from OMCT;

[3] atmospheric effect from NCEP combined with the oceanic effect from ECCO;

[4] atmospheric effect ECMWF combined with the oceanic effect from OMCT.

Results of the combinations [1], [3] and [4] are shown in the upper panels of Fig. (4) for χ_1 and of Fig. (5) for χ_2 . The signals are compared with excitation series χ_1^{geo} and χ_2^{geo} (units: as = 1000 mas) which are computed from observed polar motion (C04 series of the IERS). The relation between the excitation functions and the polar motion coordinates (x, y) (units: as) is given by

$$\chi_1^{geo} = x + \frac{2Q}{\frac{2\pi}{T_c}(1+4Q^2)}(\dot{x} + 2Q\dot{y}) \quad (10)$$

$$\chi_2^{geo} = -y + \frac{2Q}{\frac{2\pi}{T_c}(1+4Q^2)}(2Q\dot{x} - \dot{y}) \quad (11)$$

(Gross (1992)). Thereby $T_C = 433.1$ d is the Chandler period and $Q = 170$ is the so-called quality factor which accounts for the damping of the Chandler oscillation due to friction.

The correlation coefficients and RMS differences (see Fig. (6) and (7)) show that the model-only combinations [3] and [4] correspond better with geodetic observations than combinations in which satellite altimetry data are applied. Although the steric corrections are certainly not perfect, the main reason for the better agreement of [3] and [4] is, that the model-only combinations are more consistent. The phase relations between the data sets match since the ocean models are forced by the respective atmospheric data. Since the mass excitations from altimetry, the motion excitations from OMCT and the atmospheric excitations from ECMWF are not in phase, artificial signals due to the non-compensation of counteracting signals are likely. Here additional investigations are necessary.

When the hydrological effects are additionally considered (lower panels of Fig. (4) to (7)) the agreement is slightly improved in the case of LDAS. When LaD is applied the agreement gets worse. Although the influence of continental hydrology is very small it seems that LDAS reproduces continental hydrological processes better than LaD. Nevertheless the knowledge of continental hydrology is limited due to the lack of observations. Improvements can be expected from the observations of the Gravity Recovery and Climate Experiment (GRACE).

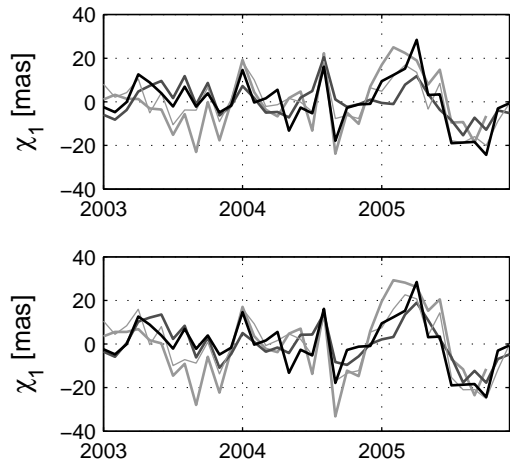


Fig. 4 Upper panel: combined atmospheric and oceanic χ_1 -components of the excitation functions (combination [1] in light-grey (fat), [3] in dark-grey (fat) and [4] in light-grey (thin)) are compared with the geodetic χ_1 -component of the excitation function (black). Lower panel: combined atmospheric, oceanic and hydrological χ_1 -components of the excitation functions (same combinations like atop plus hydrological effect from LDAS).

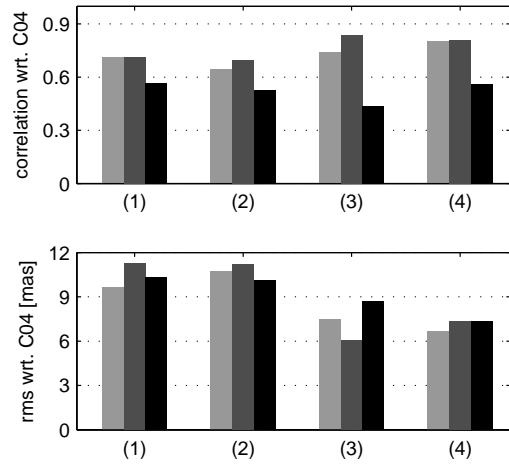


Fig. 6 Upper panel: correlation coefficients of the combined geophysical χ_1 -components of the excitation functions with respect to the geodetic observations and lower panel: corresponding RMS values (combinations [1], [2], [3] and [4] in light grey without hydrological effect, in dark grey with hydrological effect from LDAS and in black with hydrological effect from LaD).

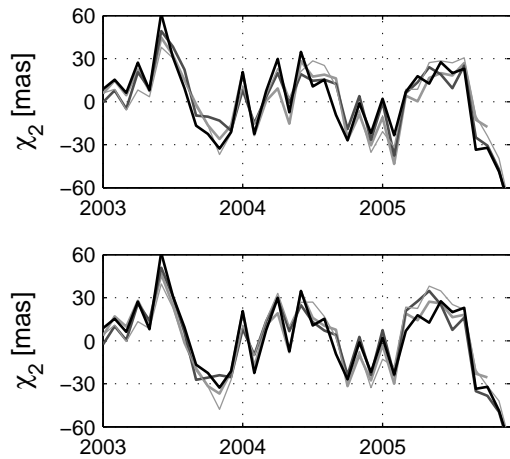


Fig. 5 Upper panel: combined atmospheric and oceanic χ_2 -components of the excitation functions (combination [1] in light-grey (fat), [3] in dark-grey (fat) and [4] in light-grey (thin)) are compared with the geodetic χ_2 -component of the excitation function (black). Lower panel: combined atmospheric, oceanic and hydrological χ_2 -components of the excitation functions (same combinations like atop plus hydrological effect from LDAS).

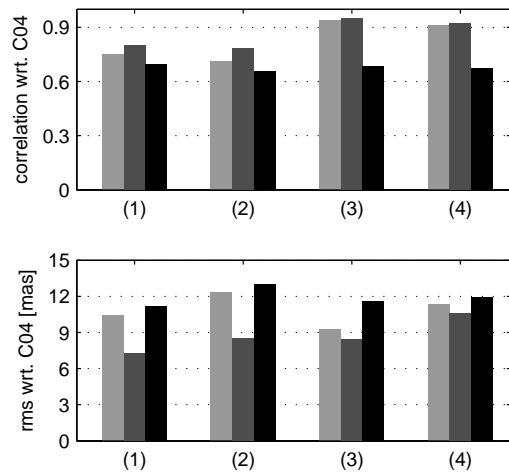


Fig. 7 Upper panel: correlation coefficients of the combined geophysical χ_2 -components of the excitation functions with respect to the geodetic observations and lower panel: corresponding RMS values (combinations [1], [2], [3] and [4] in light grey without hydrological effect, in dark grey with hydrological effect from LDAS and in black with hydrological effect from LaD).

4 Conclusions

The validation of oceanic mass excitation functions of polar motion by means of independent precise geodetic observations requires the use of geophysical data sets and models. When different data sets are combined consistency is a crucial factor. Above results showed that geophysical model-only combinations of atmospheric, oceanic and hydrological excitations agree better with geodetic observations than combinations in which satellite altimetry and physical ocean data are considered. Erroneous patterns of the atmospheric excitations are compensated by the corresponding ocean model which uses the atmospheric data as input variables. This is, of course, not the case when excitations from reduced SLA are combined with the atmospheric excitations. In order to improve the excitation functions from altimetry further investigations are necessary: On the one hand improved data sets for SLA will be derived from multi mission solutions considering the dynamic atmospheric correction (DAC) which is based on the barotropic model MOG2D (Modèle aux Oudes de Gravité - 2 dimensions). On the other hand alternative data sets for the steric correction are expected from the future Soil Moisture and Ocean Salinity satellite mission (SMOS).

Acknowledgements

This paper was developed within the subproject "Integration of Earth rotation, gravity field and geometry using space geodetic observations" of the DFG research unit FOR584 (Earth Rotation and Global Dynamic Processes). The authors thank M. Thomas for offering the OMCT and ECMWF data. NCEP reanalysis data are provided by the NOAA/OAR/ESRL PSD, Boulder, Colorado, USA. ECCO data are a contribution of the ECCO Consortium for Estimating the Circulation and Climate of the Ocean funded by the National Oceanographic Partnership Program (NOPP).

References

- Antonov, J.I., R.A. Locarnini, T.P. Boyer et al. (2006). World Ocean Atlas 2005, Volume 2: Salinity. S. Levitus, Ed. *NOAA Atlas NESDIS 62*, U.S. Government Printing Office, Washington, D.C., pp. 182
- Fofonoff, N.P. and R.C. Millard (1983). Algorithms for computation of fundamental properties of seawater, *Unesco technical papers in marine science*, 44.
- Chambers, D.P. (2006): Observing seasonal steric sea level variations with GRACE and satellite altimetry, *J. Geophys. Res.*, 111, 10.1029/2005JC002914.
- Chen, J.L., C.R. Wilson, R.J. Eanes et al. (2000). A new assessment of long-wavelength gravitational variations, *J. Geophys. Res.*, 105, 0148-0227/00/2000JB900115.
- Gross, R.S. (1992). Correspondence between theory and observations of polar motion, *Geophys. J. Int.*, 109, pp. 162-170.
- Gross, R. (2007). Earth Rotation Variations - Long Period, in: *Treatise on Geophysics*, Volume 3 - Geodesy, Elsevier, in press
- Gross, R.S., I. Fukimori and D. Menemenlis (2003). Atmospheric and oceanic excitation of the Earth's wobbles during 1980-2000, *J. Geophys. Res.*, 108, doi:10.1029/2002JB002143.
- Ishii, M., M. Kimoto, K. Sakamoto et al (2006). Steric Sea Level Changes Estimated from Historical Ocean Subsurface Temperature and Salinity Analyses, *J. Oceanography*, 62, pp. 155-170.
- Kalnay, E., M. Kanamitsu, R. Kistler et al. (1996). The NCEP/NCAR 40-year reanalysis project, *Bull. Amer. Meteor. Soc.*, 77, pp. 437-471.
- Locarnini, R.A., A.V. Mishonov, J.I. Antonov et al. (2006). World Ocean Atlas 2005, Volume 1: Temperature. S. Levitus, Ed. *NOAA Atlas NESDIS 61*, U.S. Government Printing Office, Washington, D.C., pp. 182.
- Milly, P.C.D and A.B. Shmakin (2002): Global Modeling of Land Water and Energy Balances Part I: The Land Dynamics (LaD) Model. *J. Hydrometeorology*, 3, pp. 283-299.
- Thomas, M., J. Sündermann and E. Maier-Reimer (2001). Consideration of ocean tides in an OGCM and impacts on subseasonal to decadal polar motion excitation, *Geophys. Res. Lett.*, 28(12), pp. 2457-2460.
- Zhou, Y.H., D.A. Salstein and J.L. Chen (2006). Revised atmospheric excitation function series related to Earth's variable rotation under consideration of surface topography, *J. Geophys. Res.*, 111, 10.1029/2005JD006608.